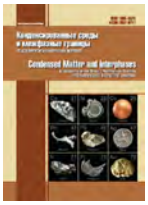

ISSN 1606-867X (Print)
ISSN 2687-0711 (Onine)
Condensed Matter and Interphases
Kondensirovannye Sredy i Mezhfaznye Granitsy
https://journals.vsu.ru/kcmf/

Original articles

Original article
https://doi.org/10.17308/kcmf.2021.23/3296

Phase relations in the Tl_2Te–$TlBiTe_2$–$TlTbTe_2$ system

S. Z. Imamaliyeva[1]✉, G. I. Alakbarzade[2], D. M. Babanly[1,3], M. V. Bulanova[4], V. A. Gasymov[1], M. B. Babanly[1]

[1]*Institute of Catalysis and Inorganic Chemistry of the Azerbaijan National Academy of Sciences, 113 H. Javid ave., Baku AZ-1143, Azerbaijan*

[2]*Azerbaijan National Aerospace Agency, 159 Azadlig ave, AZ-1106, Baku, Azerbaijan*

[3]*Azerbaijan State Oil and Industry University, French-Azerbaijani University (UFAZ), 16/21 Azadlıq prospekti, Baku AZ-1101, Azerbaijan*

[4]*Frantsevich Institute for Problems of Materials Science, NASU, 3 Krzhizhanovsky st., Kiev 03142, Ukraine*

Abstract

The phase equilibria in the Tl_2Te–$TlBiTe_2$–$TlTbTe_2$ concentration area of the Tl–Bi–Tb-Te quaternary system were investigated by using the differential thermal analysis and powder X-ray diffraction techniques. The diagram of the solid-phase equilibria of this system at room temperature was constructed. It was established that the Tl_9BiTe_6–Tl_9TbTe_6 section divides the Tl_2Te–$TlBiTe_2$–$TlTbTe_2$ system into two independent subsystems. It was found that the Tl_2Te–Tl_9BiTe_6–Tl_9TbTe_6 subsystem is characterized by the formation of a wide field of solid solutions with a Tl_5Te_3 structure (δ-phase) that occupy more than 90% of the area of the concentration triangle. The results of X-ray phase analysis of alloys of the Tl_9BiTe_6–Tl_9TbTe_6–$TlTbTe_2$–$TlBiTe_2$ subsystem showed the formation of wide regions of solid solutions based on $TlTbTe_2$ and $TlBiTe_2$ along the section of $TlTbTe_2$–$TlBiTe_2$ ((β_1- and β_2-phases) and made it possible to determine the location of the heterogeneous phase regions in this subsystem. The parameters of crystal lattices of mutually saturated compositions of the β_1-, β_2-, and δ-phases are calculated from powder diffraction patterns.

The paper also presents some polythermal sections, isothermal sections at 740 and 780 K of the phase diagram, as well as projections of the liquidus and solidus surfaces of the Tl_2Te–Tl_9BiTe_6–Tl_9TbTe_6 subsystem. The liquidus surface consists of three fields of the primary crystallization of α (Tl_2Te)-, δ- and β_1-phase. The constructed isothermal sections clearly demonstrate that the directions of the tie lines do not coincide with the T–x planes of the studied internal sections, which is characteristic of non-quasi-binary polythermal sections. The obtained new phases are of interest as potential thermoelectric and magnetic materials.

Keywords: Tl_2Te–$TlBiTe_2$–$TlTbTe_2$ system, phase equilibria, solid solutions, powder X-ray diffraction, crystal lattice, topological insulators

Acknowledgements: the work has been carried out within the framework of the international joint research laboratory "Advanced Materials for Spintronics and Quantum Computing" (AMSQC) established between the Institute of Catalysis and Inorganic Chemistry of ANAS (Azerbaijan) and Donostia International Physics Center (Basque Country, Spain) and partially supported by the Science Development Foundation under the President of the Republic of Azerbaijan, a grant EİF/MQM/Elm-Tehsil-1-2016-1(26)-71/01/4-M-33.

For citation: Imamaliyeva S. Z., Alakbarzade G. I., Babanly D. M., Bulanova M. V., Gasymov V. A., Babanly M. B. Phase relations in the Tl_2Te–$TlBiTe_2$–$TlTbTe_2$ system. *Kondensirovannye sredy i mezhfaznye granitsy = Condensed Matter and Interphases*. 2021;23 (1): 32–40. https://doi.org/10.17308/kcmf.2021.23/3296

✉ Samira Zakir Imamaliyeva, e-mail: samira9597a@gmail.com

Для цитирования: Имамалиева С. З., Алекберзаде Г. И., Бабанлы Д. М., Буланова М. В., Гасымов В. А., Бабанлы М. Б. Фазовые равновесия в системе Tl_2Te–$TlBiTe_2$–$TlTbTe_2$. *Конденсированные среды и межфазные границы*. 2021;23(1): 32–40. https://doi.org/10.17308/kcmf.2021.23/3296

1. Introduction

Binary and multinary chalcogenides of metals are of great interest as prospective materials with different functional properties such as electronic, optical, thermoelectric, topological insulators et al. [1–9].

Despite the toxicity of thallium, complex thallium chalcogenides are closely monitored as topological insulators [10–15], Weyl semimetals [16, 17], photodetectors [18, 19], X-ray and gamma radiation detectors [20, 21], as well as materials which exhibit abnormally low thermal conductivity [22–25].

Insertion to the crystal structure of chalcogenides of d- and f- elements can improve their properties and give them additional functionality, for example, the magnetic properties [26–29].

For the optimization of the functional properties of the above materials, it is necessary to plot phase diagrams of these systems, especially for the systems consisting of structural analogues, since it can be expected that they form wide areas of solid solutions [7, 30–32].

This work is a continuation of our studies on the phase equilibria in systems based on thallium-REE tellurides, in which wide areas of solid solutions with a Tl_5Te_3 structure are revealed, which are of practical interest as thermoelectric materials with anomalously low thermal conductivity [32–36]

The aim of the present work is the investigation of the solid-phase relations in the Tl_2Te–$TlBiTe_2$–$TlTbTe_2$ system.

The starting compounds and phase equilibria in the boundary systems were studied in a number of works [33, 37–43]

Tl_2Te melts congruently at 698 K [37], and has a monoclinic structure (Sp.Gr. C_2/C; a = 15.662; b = 8.987; c = 31.196Å, β = 100.76°, z = 44) [38].

$TlBiTe_2$ melts congruently at 820 K [39], and crystallizes in a hexagonal structure (Sp. Gr.R-$\bar{3}$m) with parameters a = 4.526; c = 23.12 Å; z = 3 [40].

$TlTbTe_2$ compound is structural analogue of $TlBiTe_2$ and has the following lattice parameters: a = 4.416; c = 24.27 Å; z = 3 [41].

Tl_2Te–$TlBiTe_2$ system studied by the authors of [38] is characterized by the formation of the Tl_9BiTe_6 compound which melts congruently at 830 K. This compound crystallizes in a tetragonal structure with the following lattice parameters: a = 8.855; c = 13.048 Å, z = 2 [42]. According to Ref. [39], in the Tl_2Te–Tl_9BiTe_6 system, continuous solid solutions with a morphotropic phase transition near Tl_2Te were detected. Considering that Tl_2Te and Tl_9BiTe_6 crystallize in different crystal structures, this statement seems unlikely. Therefore, the authors of [43] re-studied the phase relations in the Tl_2Te–Tl_9BiTe_6 system and showed that the system is a quasi-binary system of the peritectic type and is characterized by the formation of limited solid solutions based on the initial compounds.

Tl_2Te–$TlTbTe_2$ system was studied only in the composition interval of ⩾ 80 mol% Tl_2Te. It is shown that it is characterized by the formation of a tetragonal Tl_9TbTe_6 compound which melts with decomposition by a peritectic reaction at 780 K and has the following lattice parameters: a = 8.871; c = 12.973Å, z = 2 [35]. The Tl_2Te–Tl_9TbTe_6 subsystem is characterized by the formation of solid solutions with Tl_5Te_3 type tetragonal structure based on Tl_9TbTe_6.

In the Tl_9TbTe_6–Tl_9BiTe_6 system, continuous solid solutions based on the starting compounds were found [33].

In the $TlBiTe_2$–$TlTbTe_2$ system, it was shown that despite the isostructural character of the initial compounds, the system is characterized by the limited mutual solubility of the initial components. The solubility based on $TlBiTe_2$ reaches ~45 mol% and the solubility based on $TlTbTe_2$ is about 22 mol% [44].

2. Experimental

2.1. Materials and synthesis

Initial binary and ternary compounds were synthesized by the direct interaction of the high purity elements, all from Alfa Aesar (Germany): (thallium, CAS No 7440-28-0; tellurium, 13494-80-9; bismuth, 7440-69-9; terbium, 7440-27-9).

Tl_2Te, Tl_9BiTe_6, and $TlBiTe_2$, 10 grams each, were prepared by the melting of the elements in evacuated (~10^{-2} Pa) quartz ampoules in a single-zone electric furnace at 850 K. To

achieve an equilibrium state, after synthesis, the intermediate ingot of $TlBiTe_2$ was subjected to heat treatment 700 K for 500 h.

The synthesis of the incongruently melting compounds, Tl_9TbTe_6 and $TlTbTe_2$, was carried out by the ceramic method at 1000 K for 100 h. We used a graphitized ampoule in order to prevent the reaction of terbium with quartz. Then the ingots were slowly cooled down to room temperature, crushed in an agate mortar, pressed into pellets and the heating procedure was repeated at 900 K for 500 h.

The purity of the synthesized compounds was controlled by the differential thermal analysis (DTA) and powder X-ray diffraction (PXRD) method.

Samples of the Tl_2Te–$TlSbTe_2$–$TlTbTe_2$ system, 1 g each, were prepared by fusing pre-synthesized and identified binary and ternary compounds in evacuated quartz ampoules in a single-zone electric furnace at a temperature 30-50^0 higher than the melting temperature of the compounds, followed by cooling in a switched off furnace.

2.2. Methods

The PXRD (Bruker D8 diffractometer,CuK_α radiation) was used to control the purity of the synthesized compounds and intermediate samples. The analysis was carried out at room temperature between $10° \leqslant 2\theta \leqslant 70°$. The lattice constants were calculated by indexing of powder patterns using Topas V3.0 software.

DTA was performed using a NETZSCH 404 F1 Pegasus differential scanning calorimeter within room temperature and ~1400 K depending on the composition of the alloys at a heating rate of 10 K×min^{-1}. The temperatures of thermal effects were taken mainly from the heating curves.

3. Results and discussion

3.1. Solid-phase equilibria diagram of the Tl_2Te–$TlBiTe_2$–$TlTbTe_2$ system

Fig. 1 presents the solid-phase equilibria diagram of the Tl_2Te–$TlBiTe_2$–$TlTbTe_2$ system.

As can be seen, the stable section Tl_9BiTe_6–Tl_9TbTe_6 characterized by the formation of a continuous series of solid solutions [36] divides this system into two independent subsystems.

Tl_2Te–Tl_9BiTe_6–Tl_9TbTe_6 subsystem is characterized by the formation of a wide field of solid solutions with a Tl_5Te_3 structure (δ-phase) that occupy more than 90% of the area of the concentration triangle. Solid solutions based on Tl_2Te (α-phase) form within a narrow region. The regions of the α- and δ-phases are separated by a two-phase region α + δ. It should be noted

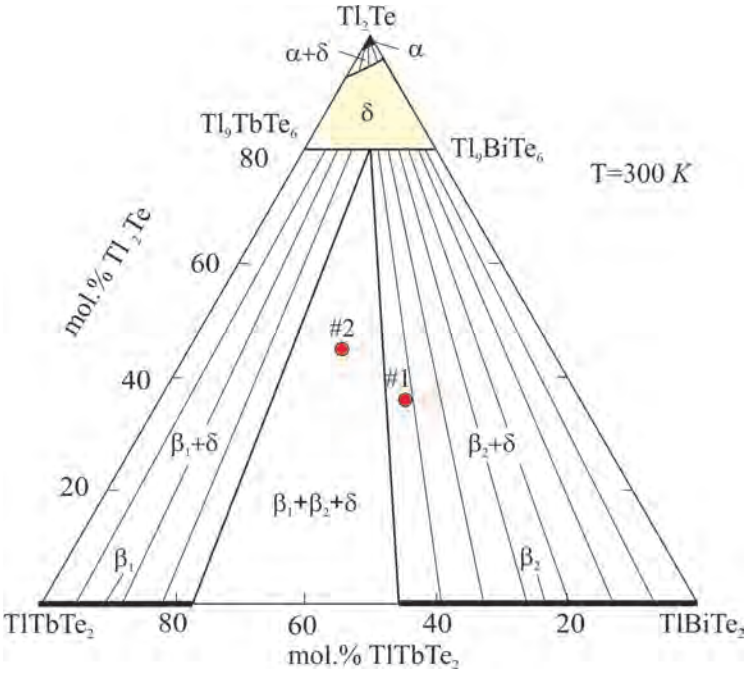

Fig. 1. The solid-phase equilibria diagram of the Tl_2Te–$TlBiTe_2$–$TlTbTe_2$ system

that a similar scheme of phase equilibria was found when studying the Tl_2Te–Tl_9BiTe_6–Tl_9ErTe_6 system [43].

While studying the Tl_9BiTe_6–Tl_9TbTe_6–$TlTbTe_2$–$TlBiTe_2$ subsystem, a number of alloys from this concentration region were investigated. Also, we used the results from our previous papers [36, 44].

The interaction of the δ-phase with solid solutions based on $TlTbTe_2$ (β_1) and $TlBiTe_2$ (β_2) leads to the formation of wide two-phase (β_1+δ and β_2+δ) fields separated by a β_1+β_2+δ three-phase area. The location and extent of the phase regions are confirmed by XRD data. As an example, Fig. 2 shows PXRD patterns from the β_1+δ two-phase (# 1) and β_1+β_2+δ three-phase (# 2) regions.

Based on the index of the PXRD patterns of the samples # 1 and # 2, we obtained the following crystal lattice parameters:

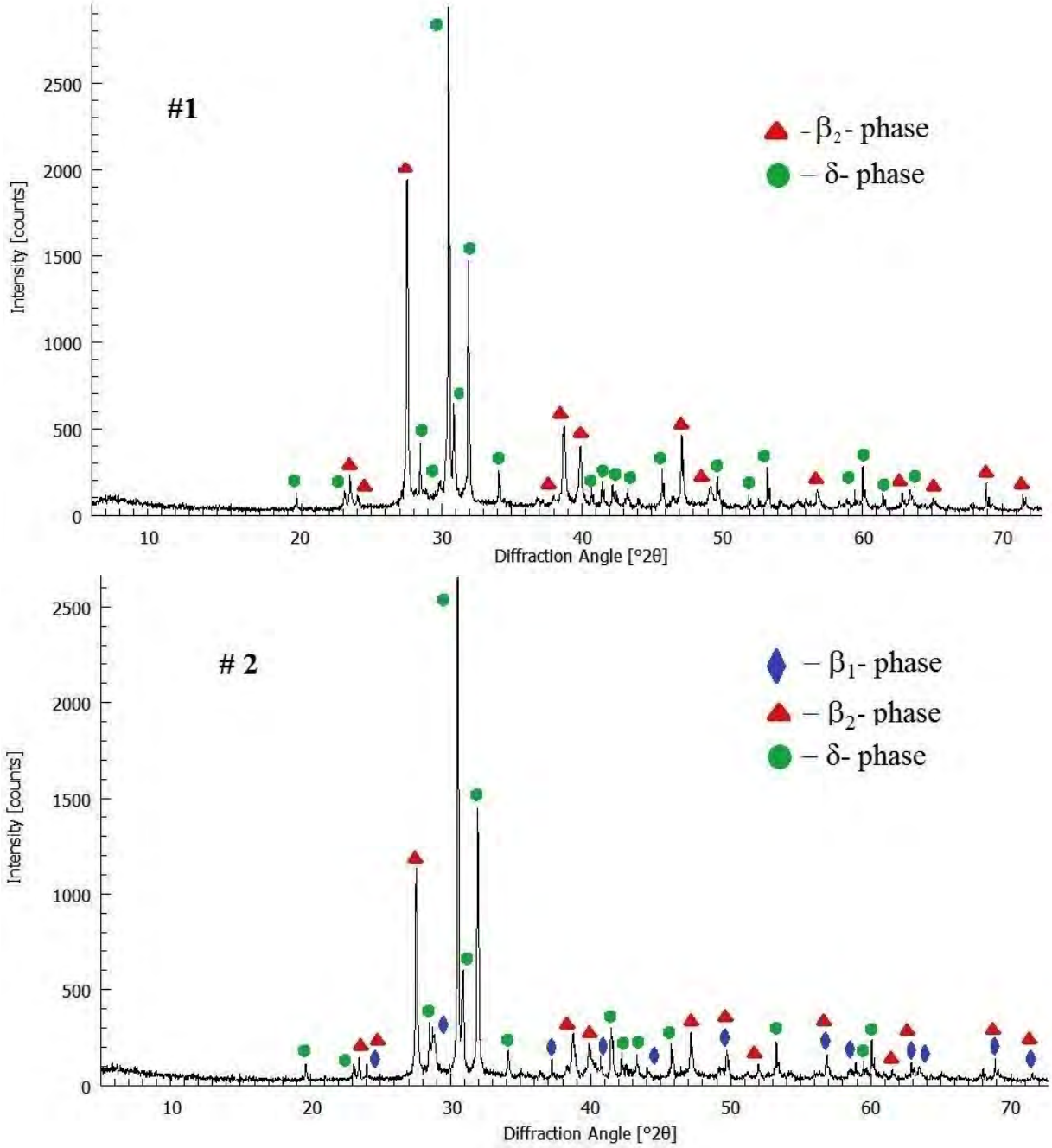

Fig. 2. The PXRD patterns of samples #1 and #2 from the two- and three-phase areas of the Tl_9BiTe_6–Tl_9TbTe_6–$TlTbTe_2$–$TlBiTe_2$ subsystem

Sample #1: a=4.4883, c=23.580 Å (β_1-phase); *a*=8.8626, *c*=13.008 Å (δ-phase)

Sample #2: a=4.4793, c=23.481Å (β_1-phase); *a*=4.4472, *c*=24.007 Å (β_2-phase); *a*=8.8630, *c*=13.005 Å (δ-phase).

A comparison of these data with the results of [36, 44] shows that sample #1 consists of a two-phase mixture of a β_1-phase with a composition of 40 mol% $TlTbTe_2$ along the section $TlBiTe_2$–$TlTbTe_2$ and a δ-phase with a composition of 50 mol% Tl_9TbTe_6 along the Tl_9BiTe_6–Tl_9TbTe_6 section. Sample #2 consist of a three-phase mixture of $\beta_1+\beta_2+\delta$ with the following phase compositions: β_1 and β_2 – respectively, 45 and 77 mol% $TlTbTe_2$ along the $TlBiTe_2$–$TlTbTe_2$ section, and δ – 50 mol% Tl_9TbTe_6. These coincide with the data in Fig. 1.

3.2. The liquidus surface of the Tl_2Te–Tl_9BiTe_6–Tl_9TbTe_6 subsystem

The liquidus surface of the Tl_2Te–Tl_9BiTe_6–Tl_9TbTe_6 system consists of three fields of the primary crystallization of the α- and δ-phases and the β_2-phase based on the $TlTbTe_2$ compound (Fig. 3). These fields are separated by p_1p_1' and p_2p_2' lines, which correspond to the $L+\beta_2 \leftrightarrow \beta$ and $L+\delta \leftrightarrow \alpha$ monovariant peritectic process. The solidus surface consists of two areas of the completion of crystallization of the α- and δ-phases.

3.3. Some polythermal and isothermal sections of the phase diagram of the Tl_2Te–Tl_9BiTe_6–Tl_9TbTe_6 subsystem

In order to confirm the correct construction of the liquidus surface of the Tl_2Te–Tl_9BiTe_6–Tl_9TbTe_6 subsystem and to refine the boundaries of areas of primary crystallization of the δ-phase and $TlTbTe_2$, the isopleth sections Tl_2Te-[A] and Tl_9TbTe_6Te-[B] (A and B – are alloys with compositions 1:1 from the boundary sections Tl_9BiTe_6–Tl_9TbTe_6 and Tl_2Te–Tl_9BiTe_6) of the phase diagram were constructed.

The liquidus curve along the Tl_2Te- [A] section consists of two curves corresponding to the primary crystallization of the α- and δ- phases. Their intersection point corresponds with the onset of the monovariant peritectic reaction $L+\delta \leftrightarrow \alpha$.

In the Tl_9TbTe_6- [B] section, in the composition range up to ~65 mol% Tl_9TbTe_6, the δ-phase crystallizes from the melt, while in the $TlTbTe_2$ – rich alloys the β_1-phase based on $TlTbTe_2$ first crystallizes, then the monovariant peritectic equilibrium $L+\beta_1 \leftrightarrow \delta$ takes place. In the latter reaction, the β_1-phase is completely consumed and the excess of melt crystallizes into the δ-phase.

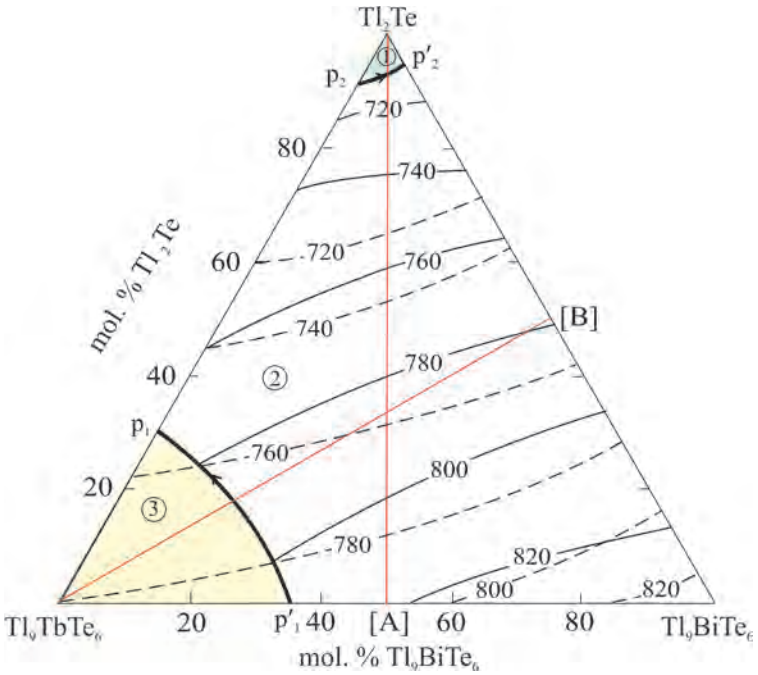

Fig. 3. Projections of the liquidus (solid lines) and solidus (dashed lines) surfaces of the Tl_2Te–Tl_9BiTe_6–Tl_9TbTe_6 subsystem. Primary crystallization fields of phases: 1 – α; 2 – δ; 3 – β_1. Red lines show the studied Tl_2Te-[A] and Tl_9TbTe_6Te-[B] polythermal sections of the subsystem

The presence of monovariant peritectic reactions $L+\beta_1 \leftrightarrow \delta$ and $L+\delta \leftrightarrow \delta$ (Fig. 3, p_2p_2' and p_2p_2 curves) in the Tl_2Te–Tl_9BiTe_6–Tl_9TbTe_6 system should lead to the formation of $L+\alpha+\delta$ and $L+\beta_1+\delta$ three-phase regions on the polythermal sections of Tl_2Te-[A] and Tl_9TbTe_6-[B], accordingly (Fig. 4). The very narrow temperature ranges of these reactions do not allow us to determine these areas by the DTA method. Taking into account the well-known principles [45] of the construction of polythermal sections, the regions $L+\beta_1+\delta$ and $L+\alpha+\delta$ in the relevant section were delimited by dashed lines.

The isothermal sections of the phase diagram are important for choosing the composition of solution-melts when growing single crystals by directional crystallization.

As can be seen, from the isothermal sections at 740 and 780 K, the first consists of conjugated liquidus and solidus curves, delimiting single-phase regions L and δ. These curves are connected by tie lines and delimit the L + δ two-phase area. The isothermal section at 780 K in addition to these phase regions, also reflects the heterogeneous regions $L+\beta_1$, $\beta_1+\delta$, and $L+\beta_1+\delta$, which are delimited taking into account data on the Tl_2Te–Tl_9TbTe_6 and Tl_2Te–Tl_9TBiTe_6 boundary systems [35, 43].

A comparison of the isothermal (Fig. 5) and polythermal (Fig. 4) sections of the phase diagram

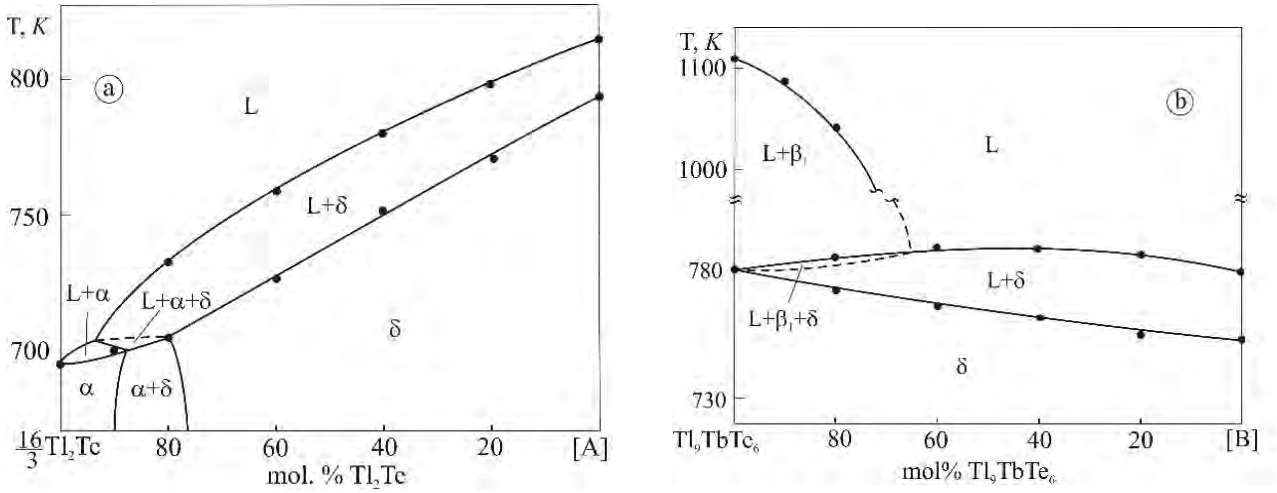

Fig. 4. Tl_2Te-[A] and Tl_9TbTe_6-[B] polythermal sections of the phase diagram of the Tl_2Te–Tl_9BiTe_6–Tl_9TbTe_6 subsystem of the Tl-Bi-Tb-Te quaternary system. A and B are equimolar compositions of the Tl_9BiTe_6–Tl_9TbTe_6 and Tl_2Te–Tl_9BiTe_6 boundary systems on Fig. 3

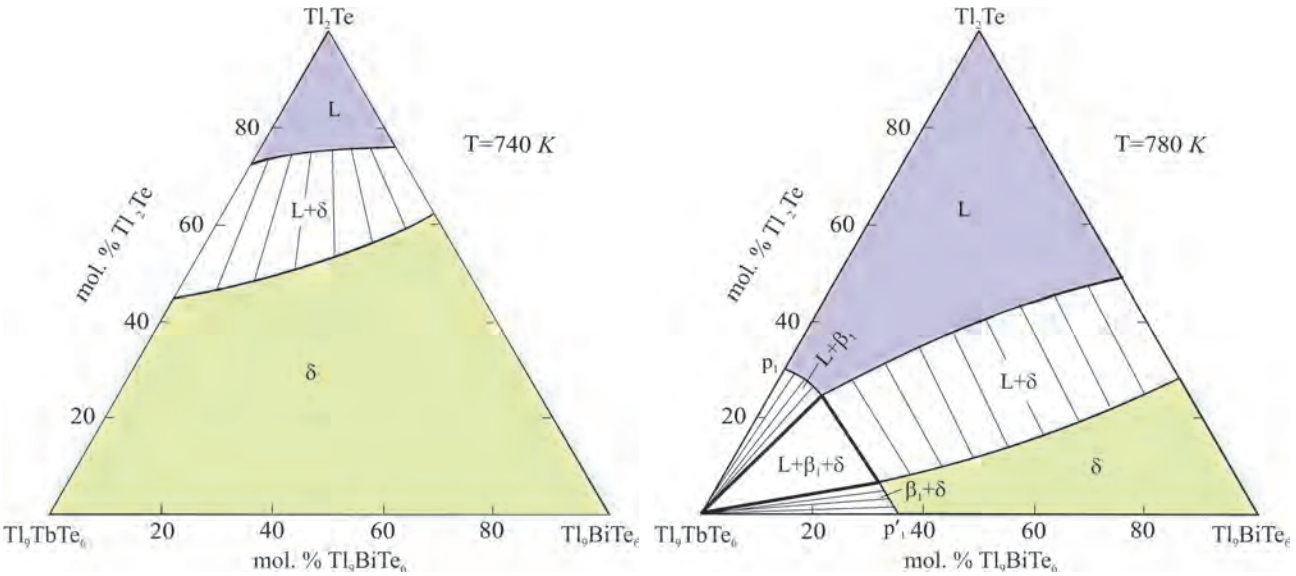

Fig. 5. Isothermal sections at 740 and 780 K of the Tl_2Te–Tl_9BiTe_6–Tl_9TbTe_6 subsystem

of the Tl_2Te–Tl_9BiTe_6–Tl_9TbTe_6 system clearly demonstrates that the directions of the tie lines do not coincide with the T–x planes of the studied internal sections, which is characteristic of non-quasi-binary polythermal sections.

4. Conclusion

The character of the solid-phase equilibria in the Tl_2Te–$TlBiTe_2$–$TlTbTe_2$ system is established by using the DTA and powder XRD. A diagram of solid-phase equilibria at room temperature of this system is constructed, as well as a number of polythermal and isothermal sections and projections of the surfaces of liquidus and solidus in the Tl_2Te–Tl_9BiTe_6–Tl_9TbTe_6 composition range. The Tl_9BiTe_6–Tl_9TbTe_6 section, characterized by the formation of a continuous series of solid solutions (δ-phase), divides the Tl_2Te–$TlBiTe_2$–$TlTbTe_2$ system into two independent subsystems. The Tl_9BiTe_6–$TlBiTe_2$–$TlTbTe_2$–Tl_9TbTe_6 subsystem is characterized by the formation of the wide areas of the solid solutions based on $TlTbTe_2$ (β_1-phase) and $TlBiTe_2$ (β_2-phase). The homogeneity region of the δ-phase covers a large (> 90% of the Tl_2Te–Tl_9BiTe_6–Tl_9TbTe_6 subsystem area). The obtained solid solutions β_1, β_2, and δ are of great interest as potential magnetic topological insulators and thermoelectric materials.

Conflict of interests

The authors declare that they have no known competing financial interests or personal relationships that could have influenced the work reported in this paper.

References

1. Ahluwalia G. K. (ed.). *Applications of chalcogenides: S, Se, and Te*. Switzerland: Springer; 2017. 461 p. https://doi.org/10.1007/978-3-319-41190-3

2. Alonso-Vante N. Outlook. In: *Chalcogenide materials for energy conversion: Pathways to oxygen and hydrogen reactions. Nanostructure Science and Technology*. Springer, Cham; 2018. 226 p. https://doi.org/10.1007/978-3-319-89612-0_7

3. Scheer R., Schock H-W. *Chalcogenide photovoltaics: physics, technologies, and thin film devices*. Wiley-VCH; 2011. 368 p. https://doi.org/10.1002/9783527633708

4. Palchoudhury S., Ramasamy K., Gupta A. Multinary copper-based chalcogenide nanocrystal systems from the perspective of device applications. *Nanoscale Advances*. 2020;2(8): 3069–3082. https://doi.org/10.1039/D0NA00399A

5. Lin S., Li W., Bu Z., Shan B., Pei Y. Thermoelectric p-type Ag_9GaTe_6 with an intrinsically low lattice thermal conductivity. *ACS Applied Energy Materials*. 2020;3(2): 1892–1898. https://doi.org/10.1021/acsaem.9b02330

6. Banik A., Roychowdhury S., Biswas K. The journey of tin chalcogenides towards high-performance thermoelectrics and topological materials. *Chemical Communications*. 2018;54(50): 6573–6590. https://doi.org/10.1039/C8CC02230E

7. Otrokov M. M., Klimovskikh I. I., Bentmann H., Zeugner A., Aliev Z. S., Gass S., Wolter A. U. B., Koroleva A. V., Estyunin D., Shikin A. M., Blanco-Rey M., Hoffmann M., Vyazovskaya A. Yu., Eremeev S. V., Koroteev Y. M., Amiraslanov I. R., Babanly M. B., Mamedov N. T., Abdullayev N. A., Zverev V. N., Büchner B., Schwier E. F., Kumar S., Kimura A., Petaccia L., Di Santo G., Vidal R. C., Schatz S., Kisner K., Min C.-H., Moser S. K., Peixoto T. R. F., Reinert F., Ernst A., Echenique P. M., Isaeva A., Chulkov E. V. Prediction and observation of the first antiferromagnetic topological insulator. *Nature*. 2019; 576(7787): 416–422. https://doi.org/10.1038/s41586-019-1840-9

8. Babanly M. B., Chulkov E. V., Aliev Z. S., Shevel'kov A. V., Amiraslanov I. R. Phase diagrams in the materials science of topological insulators based on metal chalcogenides. *Russian Journal of Inorganic Chemistry*. 2017;62(13): 1703–1729. https://doi.org/10.1134/S0036023617130034

9. Ding J., Liu C., Xi L., Xi J., Yang J. Thermoelectric transport properties in chalcogenides ZnX (X=S, Se): From the role of electron-phonon couplings. *Journal of Materiomics*. 2021;7(2): 310–319. https://doi.org/10.1016/j.jmat.2020.10.007

10. Segawa K. Synthesis and characterization of 3D topological insulators: a case $TlBi(S_{1-x}Se_x)_2$. *Science and Technology of Advanced Materials*. 2015;16(1): 014405-8. https://doi.org/10.1088/1468-6996/16/1/014405

11. Usanmaz D., Nath P., Toher C., Plata J. J., Friedrich R., Fornari M., Nardelli M. B., Curtarolo S. Spinodal superlattices of topological insulators. *Chemistry of Materials*. 2018;30(7): 2331–2340. https://doi.org/10.1021/acs.chemmater.7b05299

12. Wang Z., Segawa K., Sasaki S., Taskin A. A., Ando Y. Ferromagnetism in Cr-doped topological insulator $TlSbTe_2$. *APL Materials*. 2015;3: 083302-7. https://doi.org/10.1063/1.4922002

13. Eremeev S. V., Koroteev Y. M., Chulkov E. V. Ternary thallium-based semimetal chalcogenides $Tl–V–VI_2$ as a new class of three-dimensional topological insulators. *JETP Letters*. 2010;91(11): 594–598. https://doi.org/10.1134/S0021364010110111

14. Filnov S. O., Klimovskikh I. I., Estyunin D. A., Fedorov A., Voroshnin V., Koroleva A. V., Shevchenko E. V., Rybkin A. G., Aliev Z. S., Babanly M. B.,

Amiraslanov I. R., Mamedov N. T., Schwier E. F., Miyamoto K., Okuda T., Kumar S., Kimura A., Misheneva V. M., Shikin A. M., Chulkov E. V. Probe-dependent Dirac-point gap in the gadolinium-doped thallium-based topological insulator $TlBi_{0.9}Gd_{0.1}Se_2$. *Physical Review B*. 2020;102: 085149-7. https://doi.org/10.1103/PhysRevB.102.085149

15. Arpino K. E., Wasser B. D., McQueen T. M. Superconducting dome and crossover to an insulating state in $[Tl_4]Tl_{1-x}Sn_xTe_3$. *APL Materials*. 2015;3(4): 041507-8. https://doi.org/10.1063/1.4913392

16. Ruan J., Jian S-K., Zhang D., Yao H., Zhang H., Zhang S-C., Xing D. Ideal Weyl semimetals in the chalcopyrites $CuTlSe_2$, $AgTlTe_2$, $AuTlTe_2$, and $ZnPbAs_2$. *Physical Review Letters*. 2016;116: 226801-5. https://doi.org/10.1103/PhysRevLett.116.226801

17. Singh B., Sharma A., Lin H., Hasan M. Z., Prasad R., Bansil A. Topological electronic structure and Weyl semimetal in the $TlBiSe_2$ class of semiconductors. *Physical Review B*. 2012;86: 115208-7. https://doi.org/10.1103/PhysRevB.86.115208

18. Piasecki M., Brik M. G., Barchiy I. E., Ozga K., Kityk I. V., El-Naggar A. M., Albassam A. A., Malakhovskaya T. A., Lakshminarayana G. Band structure, electronic and optical features of Tl_4SnX_3 (X = S, Te) ternary compounds for optoelectronic applications. *Journal of Alloys and Compounds*. 2017;710: 600–607. https://doi.org/10.1016/j.jallcom.2017.03.280

19. Barchij I., Sabov M., El-Naggar A. M., AlZayed N. S., Albassam A. A., Fedorchuk A. O., Kityk I. V. Tl_4SnS_3, Tl_4SnSe_3 and Tl_4SnTe_3 crystals as novel IR induced optoelectronic materials. *Journal of Materials Science: Materials in Electronic*. 2016;27: 3901-5. https://doi.org/10.1007/s10854-015-4240-4

20. Shi H., Lin W., Kanatzidis M. G., Szeles C., Du M.-H. Impurity-induced deep centers in Tl_6SI_4. *Journal of Applied Physics*. 2017:121(14): 145102-5. https://doi.org/10.1063/1.4980174

21. Das S., Peters J. A., Lin W. W, Kostina S. S., Chen P., Kim J., Kanatzidis M. G., Wessels B. W. Charge transport and observation of persistent photoconductivity in Tl_6SeI_4 single crystals. *Journal of Physical Chemistry Letters*. 2017;8(7): 1538–1544. https://doi.org/10.1021/acs.jpclett.7b00336

22. Ding G., He J., Cheng Z., Wang X., Li S. Low lattice thermal conductivity and promising thermoelectric figure of merit of Zintl type $TlInTe_2$. *Journal of Materials Chemistry C*. 2018;6: 13269–13274. https://doi.org/10.1039/C8TC03492C

23. Shi Y., Assoud A., Ponou S., Lidin S., Kleinke H. A. New material with a composite crystal structure causing ultralow thermal conductivity and outstanding thermoelectric properties: $Tl_2Ag_{12}Te_{7+\delta}$. *Journal of American Chemical Society*. 2018;140(27): 8578–8585. https://doi.org/10.1021/jacs.8b04639

24. Han C., Sun Q., Li Z., Dou S. X. Thermoelectric enhancement of different kinds of metal chalcogenides. *Advanced Energy Materials*. 2016;6(15): 1600498-1-1600498-36. https://doi.org/10.1002/aenm.201600498

25. Heinke F., Eisenburger L., Schlegel R., Schwarzmüller S., Oeckler O. The influence of nanoscale heterostructures on the thermoelectric properties of Bi-substituted Tl_5Te_3. *Zeitschrift für anorganische und allgemeine Chemie*. 2017;643: 447–454. https://doi.org/10.1002/zaac.201600449

26. Maier S., Lefèvre R., Lin X., Nunna R., Berthebaud D., Hèbert S., Mar A., Gascoin F. The solid solution series $Tl(V_{1-x}Cr_x)_5Se_8$: crystal structure, magnetic and thermoelectric properties. *Journal of Materials Chemistry C*. 2015;3: 10509–10517. https://doi.org/10.1039/C5TC01766A

27. Guo Q., Kleinke H. Thermoelectric properties of hot-pressed (Ln = La, Ce, Pr, Nd, Sm, Gd, Tb) and $Tl_{10-x}La_xTe_6$ ($0,90<x<1,05$). *Journal of Alloys and Compounds*. 2015;630: 37–42. https://doi.org/10.1016/j.jallcom.2015.01.025

28. Isaeva A., Schoenemann R., Doert T. Syntheses, Crystal structure and magnetic properties of Tl_9RETe_6 (RE = Ce, Sm, Gd). *Crystals*. 2020;10(4): 277-11. https://doi.org/10.3390/cryst10040277

29. Bangarigadu-Sanasy S., Sankar C. R., Dube P. A., Greedan J. E., Kleinke H. Magnetic properties of Tl_9LnTe_6, Ln = Ce, Pr, Tb and Sm. *Journal of Alloys and Compounds*. 2014;589: 389–392. https://doi.org/10.1016/j.jallcom.2013.11.229

30. Villars P, Prince A. Okamoto H. Handbook of ternary alloy phase diagrams (10 volume set). Materials Park, OH: ASM International; 1995. 15000 p.

31. Babanly M. B., Mashadiyeva L. F., Babanly D. M., Imamaliyeva S. Z., Taghiyev D. B., Yusibov Y. A. Some aspects of complex investigation of the phase equilibria and thermodynamic properties of the ternary chalcogenid systems by the EMF method. *Russian Journal of Inorganic Chemistry*. 2019;64(13): 1649–1671. https://doi.org/10.1134/S0036023619130035

32. Imamaliyeva S. Z. Phase diagrams in the development of thallium-REE tellurides with Tl_5Te_3 structure and multicomponent phases based on them. Overview. *Kondensirovannye sredy i mezhfaznye granitsy = Condensed Matter and Interphases*. 2018;20(3): 332–347. https://doi.org/10.17308/kcmf.2018.20/570 (In Russ., abstract in Eng.)

33. Imamaliyeva S. Z., Alakbarzade G. I., Mahmudova M. A., Amiraslanov I. R., Babanly M. B. Experimental study of the Tl_4PbTe_3–Tl_9TbTe_6–Tl_9BiTe_6 section of the Tl–Pb–Bi–Tb–Te system. *Materials Research*. 2018;21(4): e20180189-6. https://doi.org/10.1590/1980-5373-mr-2018-0189

34. Imamaliyeva S. Z., Alakbarova G. I., Babanly K. N., Amiraslanov I. R., Babanly M. B. Tl_2Te–

Tl_9SbTe_6–Tl_9TbTe_6 system. *New Materials, Compounds and Applications*. 2018;2(3): 221–230. Available at: http://jomardpublishing.com/UploadFiles/Files/journals/NMCA/V2N3/Imamaliyeva%20et%20al.pdf

35. Imamaliyeva S. Z., Gasanly T. M., Zlomanov V. P., Babanly M. B. Phase Equilibria in the Tl_2Te–Tl_5Te_3–Tl_9TbTe_6 system. *Inorganic Materials*. 2017;53(4): 361–368. https://doi.org/10.1134/S0020168517040069

36. Imamaliyeva S. Z., Gasanly T. M., Zlomanov V. P, Babanly M. B. Phase equilibria in the Tl_5Te_3–Tl_9BiTe_6–Tl_9TbTe_6 system. *Inorganic Materials*. 2017;53(7): 685–689. https://doi.org/10.1134/S0020168517070093

37. Asadov M. M., Babanly M. B., Kuliev A. A. Phase equilibria in the system Tl–Te, *Izvestiya Akademii Nauk SSSR. Neorganicheskie Materiali*. 1977;13(8): 1407–1410. (In Russ.)

38. Cerny R., Joubert J., Filinchuk Y., Feutelais Y. Tl_2Te and its relationship with Tl_5Te_3. *Acta Crystallographica Section C*. 2002;58(5): 163. https://doi.org/10.1107/s0108270102005085

39. Babanly M. B., Azizulla A., Kuliev A. A. System Tl_2Te–Bi_2Te_3–Te. *Russian Journal of Inorganic Chemistry*. 1985;30(9): 2356–2359. (In Russ.)

40. Pradel A., Tedenac J. C., Brun G., Maurin M. Mise au point dans le ternaireTl–Bi–Te. Existence de deux phases nonstoechiometriques de type $TlBiTe_2$. *Journal of Solid State Chemistry*. 1982;5(1): 99–111. https://doi.org/10.1016/0022-4596(82)90296-1

41. Duczmal M. Structure, wlasciwosci magnetzcyne i pole krzstalicyne w potrojnzch chalkogenkach lantonowcow i talu $TlLnX_2$ (X = S, Se lub Te). Monografie. Wroclaw: Politechniki Wroclawskiej; 2003. 67 p. (In Polish)

42. Doert T., Böttcher P. Crystal structure of bismuth nonathallium hexatelluride $BiTl_9Te_6$. *Zeitschrift für Kristallographie*. 1994;209: 95. https://doi.org/10.1524/zkri.1994.209.1.95

43. Imamaliyeva S. Z., Mekhdiyeva I. F., Gasymov V. A., Babanly M. B. Tl–Bi–Er–Te system in the composition region Tl_2Te–Tl_9BiTe_6–Tl_9ErTe_6. *Russian Journal of Inorganic Chemistry*. 2019;64(7): 907–913. https://doi.org/10.1134/S0036023619070192

44. Alakbarzade G. I. Solid-phase equilibria in the $TlBiTe_2$–$TlTbTe_2$ system. *Chemical Problems*. 2019;4: 565–570. https://doi.org/10.32737/2221-8688-2019-4-565-570

45. Afinogenov Yu. P., Goncharov E. G., Semenova G. V., Zlomanov V. P. *Fiziko-khimicheskii analiz mnogokomponentnykh sistem* [Physicochemical analysis of multicomponent systems]. Moscow: MFTIB; 2006. 332 p. (In Russ.)

Information about the authors

Samira Z. Imamaliyeva, PhD in Chemistry, Assistance Professor, Institute of Catalysis and Inorganic Chemistry, Azerbaijan National Academy of Sciences, Baku, Azerbaijan; e-mail: samira9597a@gmail.com. ORCID iD: https://orcid.org/0000-0001-8193-2122.

Ganira I. Alakbarzade, PhD student, Azerbaijan National Aerospace Agency, Baku, Azerbaijan; e-mail: alakbarzadegi@gmail.com ORCID iD: https://orcid.org/0000-0001-8500-0007

Dunya M. Babanly, DSc in Chemistry, Assistance Professor, Institute of Catalysis and Inorganic Chemistry, Azerbaijan National Academy of Sciences, Azerbaijan State Oil and Industry University, Baku, Azerbaijan; e-mail: dunya.babanly@ufaz.az. ORCID iD: https://orcid.org/0000-0002-8330-7854.

Marina V. Bulanova, DSc in Chemistry, Leading Researcher, I. M. Frantsevich Institute for Problems of Materials Science, NAS of Ukraine, Kiev, Ukraine; e-mail: mvbulanova2@gmail.com. ORCID iD: https://orcid.org/0000-0002-8691-0982.

Vagif A. Gasymov, PhD in Chemistry, Assistance Professor, Institute of Catalysis and Inorganic Chemistry, Azerbaijan National Academy of Sciences, Baku, Azerbaijan; e-mail: v-gasymov@rambler.ru. ORCID iD: https://orcid.org/0000-0001-6233-5840.

Mahammad B. Babanly, DSc in Chemistry, Professor, Associate Member of the Azerbaijan National Academy of Sciences, Deputy-director of the Institute of Catalysis and Inorganic Chemistry, Azerbaijan National Academy of Sciences, Baku State University, Baku, Azerbaijan; e-mail: babanlymb@gmail.com. ORCID iD: https://orcid.org/0000-0001-5962-3710.

All authors have read and approved the final manuscript.

Received 8 January 2021; Approved after reviewing 9 February 2021; Accepted 15 March 2021; Published online 25 March 2021.

Translated by Samira Imamaliyeva
Edited and proofread by Simon Cox